View metadata, citation and similar papers at core.ac.uk

brought to you by CORE

provided by Elsevier - Publisher Connector

Cell, Vol. 106, 105–116, July 13, 2001, Copyright ©2001 by Cell Press

Transgenic Expression of Syndecan-1 Uncovers a Physiological Control of Feeding Behavior by Syndecan-3

Ofer Reizes,[1,5] John Lincecum,[1] Zihua Wang,[1] Olga Goldberger,[1] Li Huang,[1] Marko Kaksonen,[4] Rexford Ahima,[2,6] Michael T. Hinkes,[1,7] Gregory S. Barsh,[3] Heikki Rauvala,[4] and Merton Bernfield[1,5]

[1] Division of Newborn Medicine
Department of Pediatrics and Cell Biology
Harvard Medical School
300 Longwood Avenue
Boston, Massachusetts 02115

[2] Division of Endocrinology
Beth Israel-Deaconess Hospital
Harvard Medical School
Boston, Massachusetts 02115

[3] Howard Hughes Medical Institute and the Departments of Pediatrics and Genetics
Stanford University Medical Center
Stanford, California 94305

[4] Program of Molecular Neurobiology
Institute of Biotechnology and Department of Biosciences
University of Helsinki
Finland 00014

Summary

Transgenic expression in the hypothalamus of syndecan-1, a cell surface heparan sulfate proteoglycan (HSPG) and modulator of ligand-receptor encounters, produces mice with hyperphagia and maturity-onset obesity resembling mice with reduced action of α melanocyte stimulating hormone (αMSH). Via their HS chains, syndecans potentiate the action of agouti-related protein and agouti signaling protein, endogenous inhibitors of αMSH. In wild-type mice, syndecan-3, the predominantly neural syndecan, is expressed in hypothalamic regions that control energy balance. Food deprivation increases hypothalamic syndecan-3 levels several-fold. Syndecan-3 null mice, otherwise apparently normal, respond to food deprivation with markedly reduced reflex hyperphagia. We propose that oscillation of hypothalamic syndecan-3 levels physiologically modulates feeding behavior.

Introduction

Mammalian evolution has provided multiple complementary mechanisms to ensure the exquisitely precise regulation of body weight (Bray and Tartaglia, 2000; Friedman, 2000). These homeostatic controls are mostly hypothalamic systems, which detect and integrate peripheral signals and ultimately maintain energy balance by altering feeding behavior and autonomic and neuroendocrine activities (Porte et al., 1998; Schwartz et al., 2000; Spiegelman and Flier, 1996). Feeding behavior is specifically controlled by several hypothalamic neuropeptides. Antisatiety peptides enhance feeding when introduced into the brain and include agouti-related protein (Agrp), galanin, melanin concentrating hormone (MCH), neuropeptide Y (NPY), and orexin A and B, whereas satiety peptides reduce feeding and include α-melanocyte stimulating hormone (αMSH) and corticotrophin releasing hormone (CRH) (Woods et al., 1998). These peptides or their receptors are located in specific hypothalamic nuclei known to regulate energy balance. Changes in the hypothalamic level of the peptide or of its transcript in association with food deprivation, food excess, or both signify that the peptide is part of a feeding control system (Flier and Maratos-Flier, 1998; Schwartz et al., 2000).

Interactions between many signaling receptors and their ligands are modulated by secreted and/or cell surface molecules. A major group of these modulators are cell surface heparan sulfate proteoglycans (HSPGs), which bind a large number of extracellular ligands, including ECM components, growth factors, cytokines, chemokines, proteinases, proteinase inhibitors, lipoproteins, and enzymes of lipid metabolism (Conrad, 1998). The syndecans, a family of four transmembrane HSPGs in mammals, together with the members of the glypican family of glycerophosphoinositol-linked HSPGs, account for nearly all the HS that is ubiquitous at cell surfaces (Bernfield et al., 1999; Park et al., 2000). Syndecan family members are found on essentially every type of adherent cell (Bernfield et al., 1999), but are differentially expressed on distinct cell types; e.g., syndecan-1 predominates on epithelia, whereas syndecan-3 predominates on neural crest derivatives and neurons. Syndecans are induced during development, tissue injury, and in response to a variety of physiological stimuli (Bernfield et al., 1999; Hsueh and Sheng, 1999; Lauri et al., 1998).

The extracellular domains of the syndecans are released from the cell surface by cleavage of the core protein at a juxtamembrane site in a highly regulated process called ectodomain shedding (Hooper et al., 1997). The shed soluble ectodomains retain all of the HS of the parental cell surface HSPG, and thus may act in a paracrine manner, either as negative or positive effectors. Shedding of syndecan-1 and -4 ectodomains is accelerated by activation of either G protein-coupled or protein tyrosine kinase signaling receptors (Subramanian et al., 1997), which in turn activate several downstream kinases, ultimately resulting in cleavage of the core protein by a cell surface metalloprotease that is susceptible to inhibition by tissue inhibitor of metalloprotease-3 (TIMP-3) (Fitzgerald et al., 2000). Soluble syndecan ectodomains are found in vivo and are shed as part of normal turnover (Yanagishita and Hascall,

[5] Correspondence: merton.bernfield@tch.harvard.edu [M.B.]; oreizes@go.com [O.R.]

[6] Present address: Division of Endocrinology, Diabetes, and Metabolism, University of Pennsylvania School of Medicine, Philadelphia, Pennsylvania, 19104.

[7] Present Address: Neonatology Associates, 5555 Pear Tree-Dunnwoody Road, Suite 349, Atlanta, Georgia, 30342.

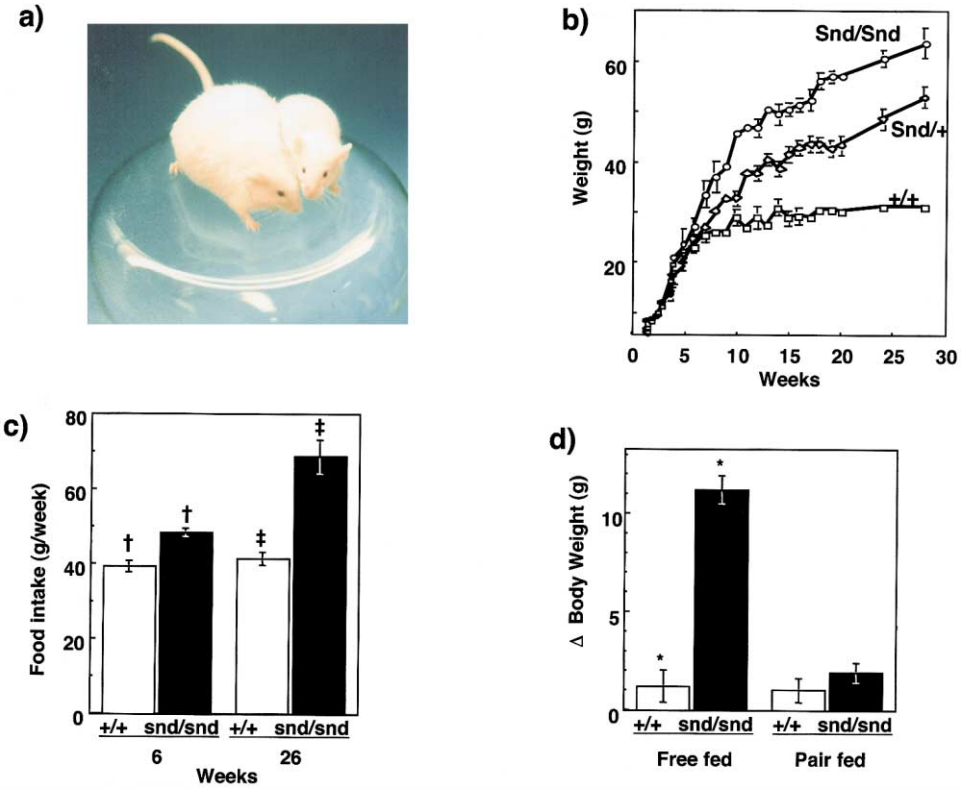

Figure 1. Syndtrophin Mice Develop Maturity-Onset Obesity due to Hyperphagia

(a) Photograph showing obese male syndtrophin mouse at six months of age and its wild-type littermate.

(b) Body weights of male syndtrophin mice (*SndA* line) on the FVB strain. Body weights were measured weekly beginning at 10 days of life. Values are mean ± SEM. *Snd/Snd* (n = 5), *Snd/+* (n = 13), and +/+ (n = 5) mice.

(c and d) Obesity in syndtrophin mice is due to hyperphagia. Mice were individually housed in metabolic chambers (c) or standard cages (d) and acclimated for one week. (c) Food and water consumption were monitored daily over a two week period. (d) Six-week-old male syndtrophin mice were pair fed an amount of chow equivalent to ad libitum fed +/+ 6-week-old male mice (5.5 g/chow day). Values are mean ± SEM, *Snd/Snd* 6 month old male (n = 5), +/+ (n = 3), 6 week old male (n = 5), and +/+ (n = 3), for pair feeding *Snd/Snd* (n = 5), and +/+ (n = 5) (†, $p < 0.05$; ‡, $p < 0.005$).

1984) and in response to pathophysiological events (Park et al., 2000).

During the course of studies of syndecan function in mice, we discovered that transgenic expression of syndecan-1 under the control of the CMV promoter/enhancer yields high levels of syndecan-1 in multiple somatic tissues and in specific regions of the brain where it is not normally expressed. Transgenically expressed syndecan-1 was found in the hypothalamic nuclei that control energy balance, and was associated with maturity-onset obesity. We named these mice syndtrophin from syndecan and from the Greek word *trofis*, meaning well fed. The obesity phenotype of syndtrophin mice closely resembled that of mice with impaired action of hypothalamic αMSH, viz agouti *lethal yellow* (A^y), transgenic agouti-related protein (Agrp), and melanocortin-4 receptor (MC-4R) null mice. Agrp (or ART), an endogenous hypothalamic peptide, competes with αMSH at the MC-3R and -4R (Ollmann et al., 1997; Shutter et al., 1997). The melanocortin receptors are seven pass transmembrane G protein-coupled receptors that stimulate adenylyl cyclase and generate the second messenger cAMP (Cone et al., 1996). Consistent with the phenotype of syndtrophin mice, we discovered that syndecan-1-bound Agrp, a hypothalamic αMSH antagonist, potentiated its activity in a cell culture system and interacted with its in vivo homolog, agouti signaling protein (ASP). Further, the transgenically misexpressed hypothalamic syndecan-1 causes obesity only when at the cell surface.

We hypothesized that transgenic misexpression of syndecan-1 in the hypothalamus mimics a physiological modulator of feeding behavior. In wild-type mice, we determined that syndecan-3, the predominantly neural member of the syndecan family, localizes in regions of the hypothalamus that control energy balance, is shed under physiological conditions, and that its level increases several-fold in response to food deprivation in a manner identical to various anti-satiety neuropeptides. Finally, syndecan-3 null mice show markedly reduced reflex hyperphagia following overnight food deprivation, directly implicating syndecan-3 in the control of feeding behavior.

Results

Generation of Syndecan-1 Transgenic Mice

Six lines of syndecan-1 transgenic mice were generated in FVB mice using the CMV promoter/enhancer. Three transgenic lines FVB/N-TgN(Synd1)aMB (denoted

Table 1. Physiological Analysis

			Glucose (mg/dl)	Insulin (ng/ml)	Leptin (ng/ml)	Corticosterone (ng/ml)
6 weeks	males	n				
	+/+	5	204 ± 21	1.2 ± 0.1	2.8 ± 0.8	nd
	Tg.Snd/Snd	5	250 ± 45	1.2 ± 0.4	3.2 ± 0.5	nd
	females					
	+/+	5	180 ± 25	1.5 ± 0.5	1.9 ± 0.4	nd
	Tg.Snd/Snd	5	190 ± 50	1.9 ± 0.4	1.8 ± 0.2	nd
6 months	males					
	+/+	6	176 ± 25*	1.1 ± 0.2‡	3.1 ± 0.2*	16.5 ± 3.0
	Tg.Snd/Snd	5	508 ± 16*	64.3 ± 19‡	17.0 ± 1.2*	20.0 ± 0.7
	females					
	+/+	7	126 ± 5†	0.4 ± 0.2†	2.5 ± 0.5†	29 ± 8.0
	Tg.Snd/Snd	6	248 ± 54†	9.4 ± 3.0	28.4 ± 5.5‡	30 ± 8.0

nd = not determined, † = $p < 0.05$, ‡ = $p < 0.005$, * = $p < 0.0001$

Tg.SndA, Tg.SndB, and *Tg.SndE*) expressed the full-length syndecan-1 cDNA, and three transgenic lines (*Tg.SndC, Tg.SndF,* and *Tg.SndG*) expressed a transgene that was identical except a stop codon was inserted 57 base pairs after the initiator methionine, resulting in a 19 amino acid truncated protein (nontranslatable control). All transgenic mice were normal at birth in litter size and morphology, and grew at a normal rate through sexual maturity. Whereas syndecan-1 is normally expressed in nearly all parenchymal tissues, and is most prominent in epithelia (Bernfield et al., 1999), the transgene was even more widely expressed. Immunohistochemical analysis of *Tg.SndA/SndA*, *Tg.SndB/+*, and *Tg.SndE/+* mice showed syndecan-1 overexpression in most epithelial tissues and misexpression in several mesenchymal tissues, including adrenal, kidney, heart and skeletal muscle, and brain. Syndecan-1 was on cell surfaces in these tissues with the exception of heart and skeletal muscle where staining was intracellular. Syndecan-1 protein expression in tissues from nontranslatable control lines *Tg.SndC/SndC, Tg.SndF/+,* and *Tg.Snd/G+* was identical to that in wild-type mice.

Transgenic Expression of Syndecan-1 Leads to Maturity-Onset Obesity

At approximately 8 weeks, both homozygote and hemizygote *Tg.SndA* line mice begin to show increased body weight (Figures 1a and 1b). While wild-type (+/+) mice plateau in weight, the transgenic mice continue to gain weight throughout life, although at a reduced rate beyond six months of age. Hemizygotes showed a weight gain intermediate between homozygotes and wild-type mice. The two additional lines (*Tg.SndB* and *Tg.SndE*) showed similar growth profiles (data not shown). Lines containing the nontranslatable syndecan-1 transgene (*Tg.SndC, Tg.SndF,* and *Tg.SndG*) did not become obese (data not shown). Because only data from the *Tg.SndA* line are presented here, *Snd/+* and *Snd/Snd* will be used to denote hemizygote and homozygote transgenic mice, respectively.

Weight gain in syndrophin mice is predominantly due to hyperphagia. Ad libitum food consumption was measured over a two week period in *Snd/Snd* and control mice at 6 weeks and 6 months of age (Figure 1c). At 6 weeks of age, food consumption in males was 23% and females 17% greater than their control littermates, while at 6 months, food consumption in males was 78% and females 70% greater than their control littermates. These mice feed continuously, even during daylight hours. Pair feeding studies were undertaken to evaluate the contribution of food intake to weight gain (Figure 1d). Six-week-old *Snd/Snd* male mice were fed a diet equivalent to their +/+ littermates (5.5 g chow per day) for 2 weeks. While *Snd/Snd* mice on an unrestricted diet continued to gain weight, their food restricted partners showed no significant increase in weight. The lack of weight gain on a pair fed diet suggests that the weight gain is primarily due to hyperphagia.

Syndrophin mice accumulate fat in all adipose tissue depots as visualized by magnetic resonance imaging (data not shown). Carcass analysis indicated that the increased weight was due to accumulation of neutral fat. *Snd/Snd* males contained 2.5-fold more triglyceride while females contained 2.9-fold more triglyceride than controls. Although the amount of total protein in the transgenic mice was increased (data not shown), total protein as a proportion of body weight was the same as in the wild-type mice. All organs showed increased weight but only adipose tissue showed an increase that was proportionately greater than the increase in body weight. *Snd/Snd* mice showed a 10% increase in overall body length (data not shown). The proportional increases in organ weights and total protein and the increased length suggest that lean body mass is not affected in these mice.

Syndrophin mice show increased plasma leptin, insulin, and glucose levels (obese males) but normal corticosterone levels (Table 1). Glucose, insulin, and leptin levels at 6 weeks were normal but obese (6 month) *Snd/Snd* males were hyperinsulinemic and hyperglycemic, with glucose levels exceeding 500 mg/dl. Leptin levels correlated with the extent of obesity; levels were 5-fold over controls in males and greater than 10-fold in females (Table 1). The syndrophin mouse phenotype, including adult onset obesity, relatively unchanged lean body mass, increased linear growth, generalized fat distribution, and blood chemistry, is distinct from that seen in *ob/ob* and *db/db* mice. Syndrophin mice mimic the phenotype seen in agouti A^y/a, Tg.Agrp, MC-4R null, and POMC null mice obesity syndromes, suggesting the same underlying etiology, viz impaired hypothalamic αMSH signaling. (Huszar et al., 1997; Ollmann et al., 1997; Yaswen et al., 1999; Yen et al., 1994).

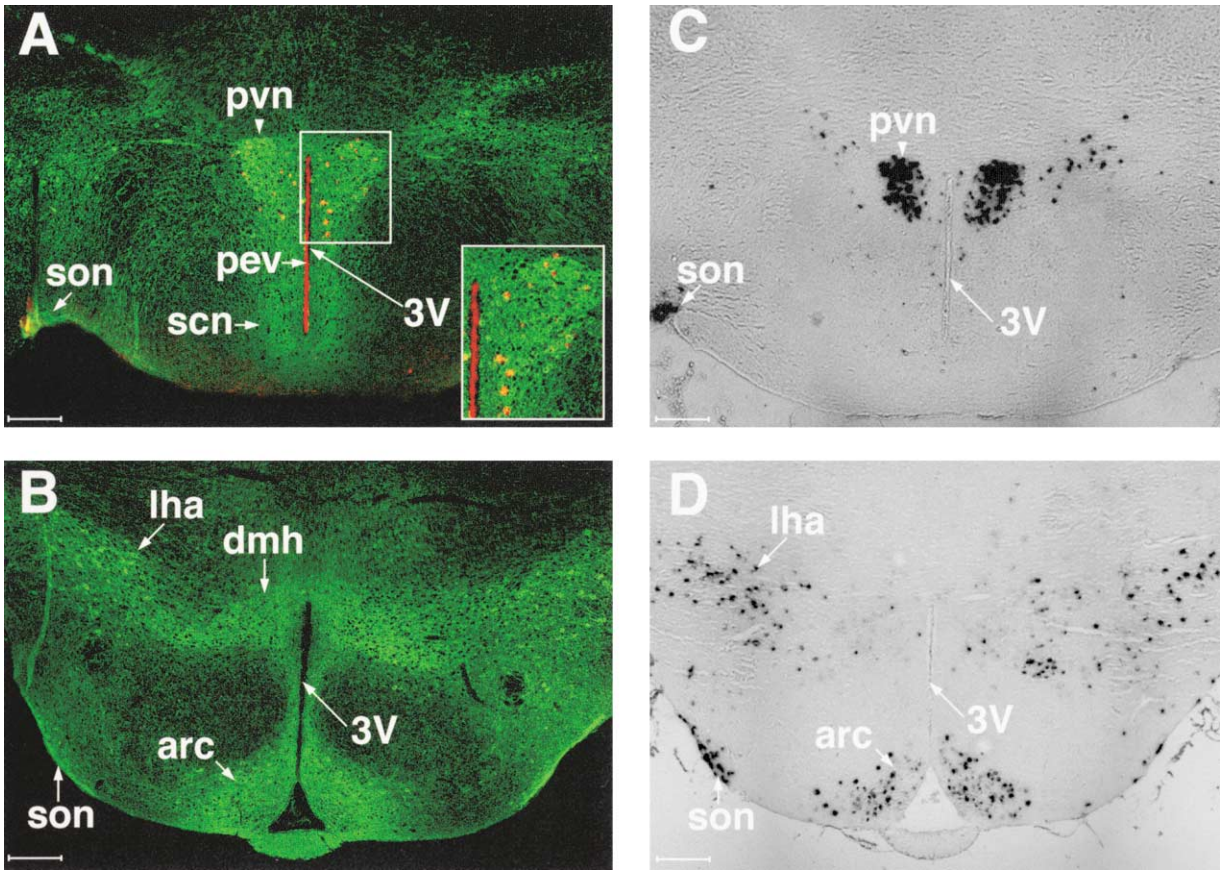

Figure 2. Syndecan-1 Is Expressed in Hypothalamic Nuclei of Syndtrophin Mice

Protein and transcript expression patterns of syndecan-1 in the hypothalamus of *Snd*/*Snd* (*SndA* line) 6-month-old mice. (A) and (B) are confocal images of coronal sections from *Snd*/*Snd* mice processed for double immunohistochemical labeling of syndecan-1 protein expression (green) and the hypothalamic paraventricular nuclei marker oxytocin (red). (A) inset shows magnification of paraventricular nuclei. (C) and (D) are serial sections processed for in situ hybridization using an antisense riboprobe specific for the syndecan-1 transcript. Representative sections were taken from the anterior (A and C) or posterior (B and D) hypothalamus. arc, arcuate; dmh, dorsomedial hypothalamus; lha, lateral hypothalamic area; pev, periventricular nuclei; pvn, paraventricular nuclei; scn, suprachiasmatic nuclei; son, supraoptic nuclei; and 3V, third ventricle. Scale bar = 250 μm.

Syndtrophin Mice Express Syndecan-1 in the Hypothalamic Nuclei that Regulate Feeding and Energy Balance

Due to the phenotypic similarity of syndtrophin mice to mice with impaired hypothalamic αMSH signaling, we evaluated the expression pattern of the wild-type gene and the transgene in the brain. Immunohistochemical and in situ hybridization of +/+ mice showed no endogenous syndecan-1 protein or mRNA expression in the brain (data not shown). However, both syndecan-1 protein and mRNA were in the brains of syndtrophin mice, essentially limited to certain hypothalamic nuclei and their projections (Figure 2). Identical expression patterns were seen in 6-week- and 6-month-old mice as well as in *Tg.SndB*, and *Tg.SndE* lines. Anteriorly, syndecan-1 was expressed in the paraventricular, suprachiasmatic, and supraoptic nuclei (Figures 2A and 2C), and posteriorly in the dorsomedial, arcuate, and lateral area hypothalamic nuclei (Figures 2B and 2D). Staining with oxytocin confirms that syndecan-1 localized to the paraventricular nuclei anteriorly (Figure 2A) (Paxinos, 1995). Oxytocin immunoreactivity was also detected in the periventricular nuclei. Syndecan-1 staining was observed on the surfaces of cell bodies and along fiber tracts (e.g., central nuclei of the amygdala, paraventricular thalamic nuclei, median eminence, and the olfactory bulb) (data not shown). Syndecan-1 mRNA was detected only in the hypothalamus, and in an identical distribution as the protein (Figures 2B and 2D). This expression was not associated with morphological or light microscopically identifiable histological abnormalities. The nontranslatable syndecan-1 transgene expressed syndecan-1 mRNA in the same hypothalamic nuclei as the *Snd*/*Snd* mice (data not shown), indicating that the hypothalamic localization of the mRNA is not secondary to the obesity phenotype.

Syndecans Modulate the Activity of AGRP and ASP

The phenotype and the hypothalamic localization of the transgene suggested an interaction between syndecan-1 and a component of the αMSH signaling pathway. Thus, a ligand blot assay (Salmivirta et al., 1991) was used to assess whether syndecan-1 interacts directly with

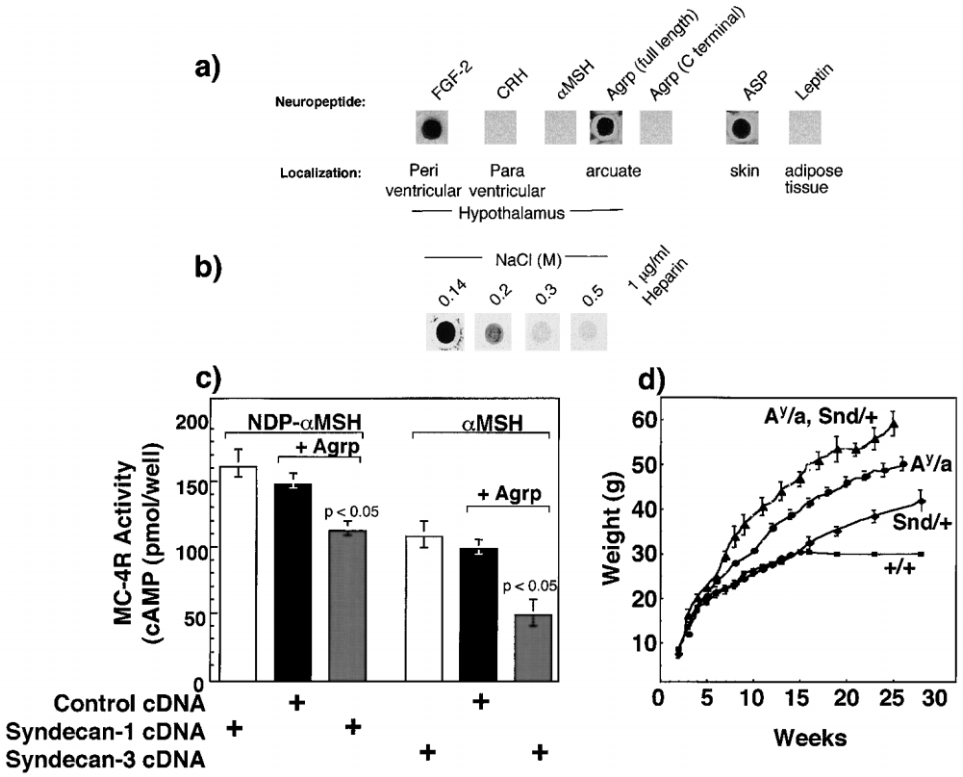

Figure 3. Syndecan-1 HS Chains Bind and Potentiate the Activity of Agouti-Related Protein (Agrp) and Agouti Signaling Protein (ASP)

(a) Syndecan-1 binds to ASP and Agrp via its N-terminal region. Five nmol of FGF-2, Agrp (full-length), Agrp (C-terminal, approximately 50 amino acids), ASP (full length) as well as α-melanocyte stimulating hormone (αMSH), corticotropin releasing hormone (CRH), and leptin were bound to nitrocellulose membranes. Blots were incubated overnight at 4°C with [^{35}S]syndecan-1 ectodomain, washed in PBS, dried, and exposed for autoradiography.

(b) Via its HS chains, syndecan-1 interacts with Agrp under physiological salt conditions. Five nmol Agrp was bound to a nitrocellulose membrane, incubated with [^{35}S]syndecan-1 ectodomain in PBS at varying NaCl concentrations or with heparin (1000 ng/ml), and blots processed as above.

(c) Cell surface syndecan-1 or -3 potentiate the action of Agrp. HEK293 cells expressing the human MC4-R were transiently transfected with either syndecan-1, -3, or control (nontranslatable syndecan-1) cDNAs. To evaluate the effects of the syndecans, cells were incubated for 30 min with Agrp (1 nM), a suboptimal concentration to inhibit αMSH or its stable analog NDP-αMSH, then stimulated for 30 min with varying concentrations of αMSH and assayed for generation of cAMP. Data shown are for 100 nM αMSH or NDPαMSH and presented as mean ± SEM (n = 3).

(d) Syndecan-1 potentiates the obesity of *lethal yellow* (*Aʸ/a*) mice. The syndecan-1 transgene was backcrossed into C57Bl/6J mice for 7 generations then intercrossed with *Aʸ/a* mice. Values are mean ± SEM. *Aʸ/a,Snd/+* (n = 5), *Aʸ/a* (n = 6), *Snd/+* (n = 6), and *+/+* (n = 5).

known components of this pathway. Soluble syndecan-1 ectodomain from NMuMG cells was used because its HS chains are similar in size (approximately 35 kDa) (Jalkanen et al., 1985) to hypothalamic syndecan-1 from syndtrophin mice and to brain syndecan-3 from wild-type mice (Figures 4b and 5b). Syndecan-1-bound FGF-2, but also ASP, and Agrp, but not NPY, leptin, MCH, CRH, and importantly, αMSH (Figure 3a and data not shown). Agrp (full-length, but not C-terminal domain) and ASP both bind in a heparin- and salt-dependent manner (Figures 3a and 3b). The affinity of the interaction could not be estimated because of limiting amounts of full-length Agrp.

Agrp is a competitive antagonist of αMSH at the melanocortin-3R and -4R (Ollmann et al., 1997). αMSH binding to these receptors results in adenylyl cyclase activation and generation of intracellular cAMP. Ten to one hundred nM Agrp competitively inhibits αMSH binding, resulting in reduced cAMP accumulation. To evaluate whether cell surface syndecans modulate this inhibition of the MC-4R by Agrp, we transfected HEK 293 cells expressing hMC-4R (Lu et al., 1994; Ollmann et al., 1997) with syndecan-1, -3 (the neural syndecan), or control cDNA (containing nontranslatable syndecan-1 cDNA). MC-4R activity was unaffected by the transfections or by 1 nM concentration of Agrp (data not shown). To evaluate the effects of cell surface syndecans, the transfectants were treated with 100 nM αMSH or its stable analog NDP-αMSH (100 nM), and assayed for cAMP generation in the presence or absence of 1 nM Agrp, a concentration which does not affect αMSH action in this assay. However, cells transfected with syndecan-1 or -3 showed significant inhibition of MC-4R activity (Figure 3c), suggesting that cell surface syndecans can potentiate the action of Agrp in cultured cells.

Analogously, transgenically expressed syndecan-1 potentiates the action of ASP in vivo in double mutant *Aʸ/a, Snd/+* mice. C57Bl6J-Snd/+(N7) mice develop

obesity less quickly than when the transgene is on the FVB background; weight gain does not exceed that of +/+ mice until 15–16 weeks (Figure 3d). Weight gain in the *A^y/a* mice becomes abnormally rapid at approximately 6 weeks. However, the double mutant (*A^y/a, Snd*/+) mice begin to show increased weight gain at approximately 4 weeks, and their weight gain prior to 16 weeks exceeds the sum of the weight gained by the parental strains. Thus, mice bearing the syndecan-1 transgene gain weight more rapidly and to a greater extent in *A^y/a* than in +/+ mice, suggesting that transgenic syndecan-1 potentiates the obesity-inducing action of hypothalamic ASP in vivo.

Cell Surface but Not Shed Syndecan-1 Produces Obesity

Syndecan-1 in most tissues is in two pools, one at the cell surface and extractable solely with detergent, the other shed as the soluble ectodomain and extractable in the absence of detergent (Figure 4a). Hypothalamic syndecan-1 in syndtrophin mice is solely extracted by detergent and is not soluble (Figure 4b). After removal of the GAG chains, hypothalamic syndecan-1 migrates as a single band (~80 kDa), while skin syndecan-1 migrates as a double band, the smaller of which is the soluble ectodomain (69 kDa) (Fitzgerald et al., 2000; Subramanian et al., 1997). These data indicate that in syndtrophin mice, a proportion of skin syndecan is the shed, soluble syndecan-1 ectodomain, and that hypothalamic syndecan-1 is not shed.

Additional transgenic lines were generated to evaluate the significance of ectodomain shedding: An uncleavable (UC) syndecan-1 was made by swapping the juxtamembrane 15 amino acids (E^{238}GATGASQSLLDTKE^{252}) of syndecan-1 with human CD4, which prevents shedding, and a constitutively shed (CS) syndecan-1 was made by inserting a stop codon in the juxtamembrane domain at amino acid Q245 (O.R., unpublished data). These mutant constructs were tested by transfection into CHO cells and shown to behave precisely as designed (Fitzgerald et al., 2000; data not shown). Several lines of transgenic mice were generated on the FVB strain and three lines of each, shown by immunohistochemical analyses to localize the transgene identically as in syndtrophin mice, were selected for study (Figure 4c). Western analyses indicated that in the hypothalamus, the UC transgene expressed less well and the CS transgene better than the syndecan-1 transgene (data not shown). Mice expressing the UC construct began to gain weight excessively at 6 weeks, while the CS mutants failed to become obese, gaining weight identically as their wild-type littermates. Thus, hypothalamic syndecan-1 generates obesity solely when at the cell surface.

Syndecan-3 Is Expressed in Hypothalamus and Regulated by Feeding State

Transgenic syndecan-1 misexpressed in the hypothalamus causes hyperphagia apparently by potentiating the action of Agrp on MC-4R. We considered the possibility that the transgenic syndecan-1 interfered with a normally functioning modulator of feeding behavior, and evaluated whether syndecan-3, known to be in the brain,

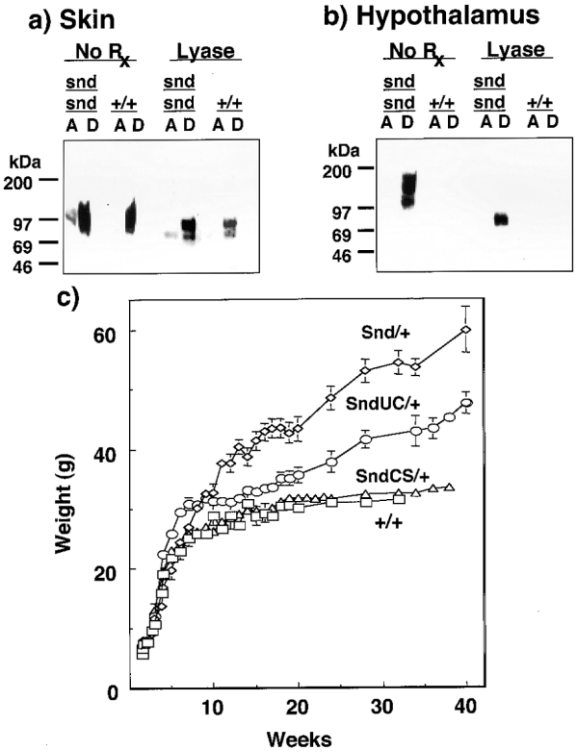

Figure 4. Cell Surface Syndecan-1 in Hypothalamus Leads to Obesity

(a and b) Syndecan-1 is expressed at the cell surface and as a soluble ectodomain in the skin (a) and solely at the cell surface in the hypothalamus (b) of syndtrophin mice. Aqueous (A) or detergent extracts (D) of *Snd/Snd* or +/+ mice were either untreated (No R_x) or digested with heparin lyase I, heparin lyase III, and chondroitinase ABC (Lyase). Samples were blotted with anti-syndecan-1 monoclonal antibody. Approximately 5 μg total protein was applied per lane.

(c) Cell surface expression of syndecan-1 results in obesity. Mutant syndecan-1 cDNAs that code for solely a cell surface/uncleavable (SndUC) syndecan-1 or a constitutively shed/secreted (SndCS) syndecan-1 were generated in FVB mice. Mutant mice were genotyped as above and weight monitored weekly for 40 weeks. Data shown are for the hemizygotes SndUC/+ (n = 10), SndCS/+ (n = 10), Snd/+ (n = 13), and wild-type +/+ (n = 6).

could be the physiological analog of misexpressed syndecan-1.

Immunostaining showed syndecan-3 in the hypothalamus of +/+ mice (Figure 5a). Anteriorly, syndecan-3 was expressed in the paraventricular hypothalamic nuclei (panel A), and posteriorly in the lateral area hypothalamic nuclei (panel C). Paraventricular staining was confirmed by staining adjacent sections for oxytocin (panel B), though oxytocin staining was also observed in the periventricular nuclei (Paxinos, 1995). The syndecan-3 is detected on the surfaces of neuronal cell bodies and projections (data not shown). Staining was blocked by preincubation with a GST-syndecan-3 fusion protein (data not shown). Western analysis indicated that the size of the syndecan-3 HS chains are indistinguishable from those on hypothalamic syndecan-1 in syndtrophin mice. In contrast to hypothalamic transgenic syndecan-1, one-third of hypothalamic syndecan-3 was soluble, and the remainder was sedimentable, suggesting both shed

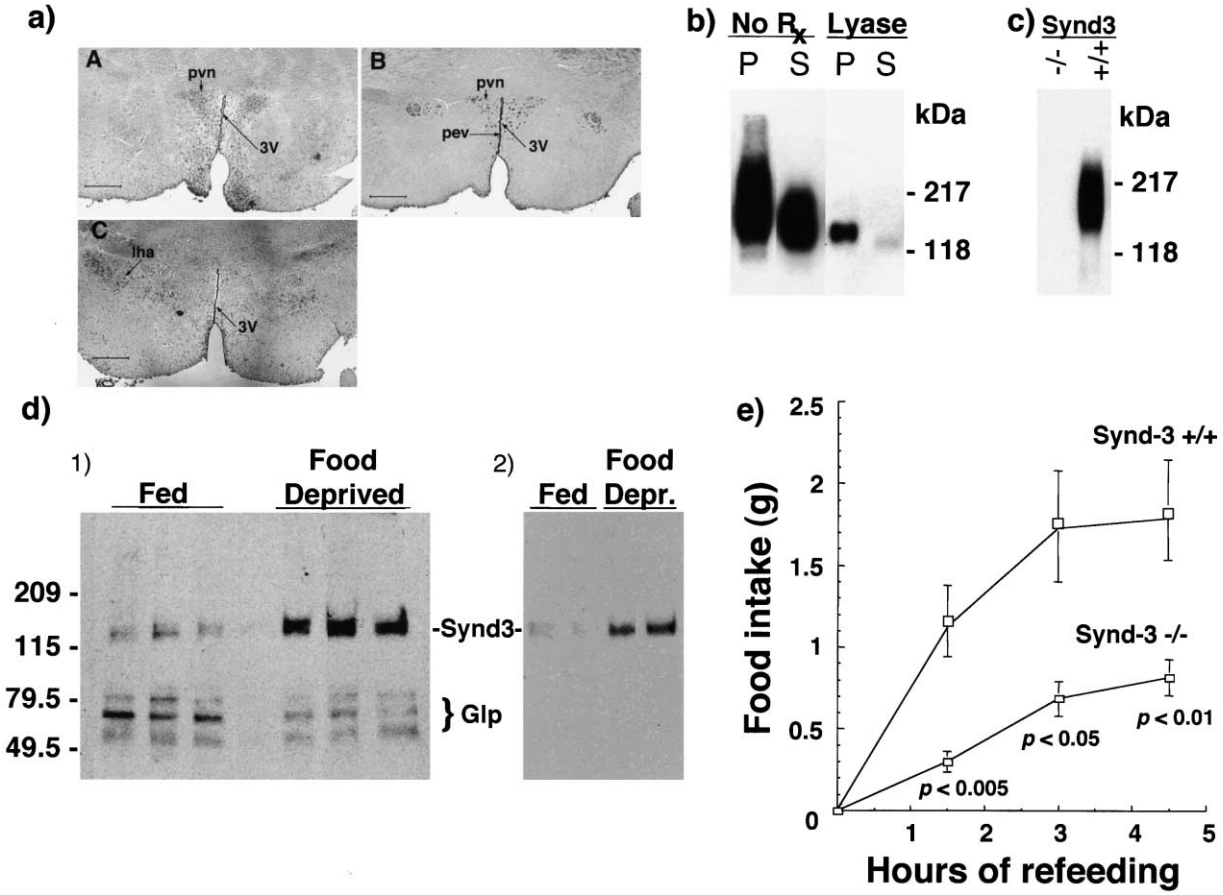

Figure 5. Syndecan-3 Modulates Feeding Behavior in Wild-Type Mice

(a) Syndecan-3 is normally expressed in hypothalamic nuclei that regulate feeding behavior. Immunohistochemical analysis of syndecan-3 and oxytocin protein expression in the hypothalamus of 3-month-old (+/+) mice. Data presented are representative section from the anterior (panels A and B) or posterior (panel C) hypothalamus. Panel B is an adjacent section to Panel A and demonstrates expression of the anterior hypothalamic marker oxytocin. lha, lateral hypothalamic area; pev, periventricular nuclei; pvn, paraventricular nuclei; 3V, third ventricle. Scale bar = 250 μm.

(b) Syndecan-3 in the hypothalamus of +/+ mice is comprised of both intact transmembrane HSPG and soluble ectodomain. Soluble (100,000 × g supernatants, S) or membrane bound (100,000 × g pellets, P) HSPGs were either untreated (No R_x) or digested with heparin lyase II and chondroitinase ABC (Lyase). Samples were blotted with affinity-purified syndecan-3 specific antibody. Approximately 5 μg total protein was applied per lane.

(c) Syndecan-3 null mice have no detectable syndecan-3 proteoglycan. Hypothalamic PGs from 3-month-old syndecan-3 (synd-3) null (−/−) and +/+ mice were partially purified by the phenol/GuHCl method, and blotted using affinity-purified mouse syndecan-3 antibodies.

(d) Hypothalamic syndecan-3 levels increase in response to food deprivation. Six-week-old C57Bl/6J male mice were either fed ad libitum or food-deprived for 24 hr with free access to water. The mice were then sacrificed, each hypothalamus rapidly removed, and individually extracted. The proteoglycans were partially purified using phenol/GuHCl method, digested with heparin lyase II and chondroitinase ABC, and the HSPGs analyzed by Western analysis using (1) mAb 3G10, which reacts with a lyase-produced HS epitope on HSPG core proteins, or (2) affinity purified antibody specific for mouse syndecan-3.

(e) Syndecan-3 null mice show diminished reflex hyperphagia compared to their control +/+ littermates. Three month old male syndecan-3 null and wild-type littermates were individually housed and acclimatized for a one week period. Mice were weighed and food deprived for 16 hr beginning with the onset of the dark cycle. The next day, mice were weighed, a preweighed amount of chow was provided, and chow weighed at the indicated times. Data presented are mean ± SEM, syndecan-3 null (n = 7) and +/+ (n = 5), and are combined from two independent experiments.

ectodomain and membrane-bound forms of syndecan-3 (Figure 5b).

We hypothesized that if hypothalamic syndecan-3 is physiologically involved in regulating feeding behavior, its level would change with feeding as do various hypothalamic peptides that modify feeding behavior (Schwartz et al., 2000). Hypothalamic HSPGs extracted from unrestricted and food deprived (24 hr) wild-type C57Bl/6J mice were heparin-lyase treated, subjected to PAGE, and detected by either an antibody specific for the heparin lyase generated epitope, mAb 3G10 (Figure 5d panel 1) or an affinity-purified syndecan-3 antibody (Figure 5d, panel 2). The bands detected correspond in PAGE mobility to syndecan-3 and to various glypicans; no other HSPGs were detected (Figure 5d, panel 1). Remarkably, food deprivation increased hypothalamic syndecan-3 levels more than 4-fold above that of ad libitum fed mice, while the levels of the putative glypi-

Table 2. Induction of Hypothalamic Syndecan-3 Expression by 24 hr Food Deprivation

	Change in proteoglycan level* Food Deprived/Fed	
	Syndecan-3	Glypicans
Experiment 1†	4.6 ± 0.9 (n = 5)[1]	0.5 ± 0.1 (n = 5)
Experiment 2‡	3.2 ± 0.9 (n = 4)[2]	0.9 ± 0.2 (n = 4)

*Summary of data presented in Figure 5c† and other data‡ quantitated from mAb 3G10 antibody immunoblots.
[1]$p < 0.05$, [2]$p < 0.005$

cans were unchanged (Table 2). The elevated levels of syndecan-3 fall with refeeding (data not shown). Because the GAG-free soluble ectodomain binds poorly to the cationic membrane used for the blots, the levels seen here predominantly represent cell surface syndecan-3. Thus, hypothalamic cell surface syndecan-3 levels change with food deprivation and refeeding in a manner similar to Agrp and other hypothalamic modifiers of feeding behavior.

Because syndecan-3 is induced upon food deprivation, we evaluated whether its loss, in null mice, would modulate feeding behavior. Syndecan-3 null mice are viable, born in expected Mendelian ratios, are healthy, and show no apparent morphological, histological, or behavioral abnormalities. However, they exhibit marked changes in hippocampal long-term potentiation and in spatial memory. These mice will be described in a separate publication (M.K., I. Pavlov, V. Voikar, S. Lauri, A. Heinola, M. Lasko, T. Taira, and H.R.). Supplemental information on the generation of the mice is available on the Cell website at http://www.cell.com/cgi/content/full/106/1/105/DC1). Additionally, we determined that no syndecan-3 was detected in the hypothalamus of syndecan-3 null mice (Figure 5c). To evaluate the role of syndecan-3 on feeding behavior, male three-month-old syndecan-3 null mice and +/+ littermates (29.6 g ± 0.8 g, n = 7, and 30.5 g ± 0.1 g, n = 5, respectively) were food deprived for 16 hr, weighed, refed, and food consumption monitored (Figure 5e). The rate and extent of reflex hyperphagia in the syndecan-3 null mice was significantly reduced compared to their +/+ littermates. The reduced hyperphagia in syndecan-3 null mice was not due to differential weight loss during food deprivation (approximately 3 g in both groups).

Discussion

Our finding that transgenically expressed hypothalamic syndecan-1 causes hyperphagia and obesity has uncovered a physiological role for syndecan-3 in the modulation of feeding behavior. We find that syndecan-3 is expressed in hypothalamic feeding centers, is both at the cell surface and shed as the soluble ectodomain, its levels change in response to food deprivation, and its deficiency results in markedly reduced reflex hyperphagia after food deprivation. Our results add syndecan-3 to the panoply of factors involved in the control of body weight. This multiplicity of regulatory peptides and receptors likely reflects the evolutionary importance of body weight maintenance, but can obscure the effects of manipulating any single signaling system (Palmiter et al., 1998).

Transgenic expression of syndecan-1 results in obese mice that resemble mice with reduced action of αMSH. In these mice, obesity develops after they reach maturity, corticosterone levels are normal, lean body mass is unaffected, and body size slightly larger than in wild-type mice (Yen et al., 1994). Moreover, the syndecan-1 transgene is expressed in a pattern similar to MC-4R and Agrp neurons and their projections (Bagnol et al., 1999; Mountjoy et al., 1994). This hypothalamic expression pattern may result from the presence of a binding

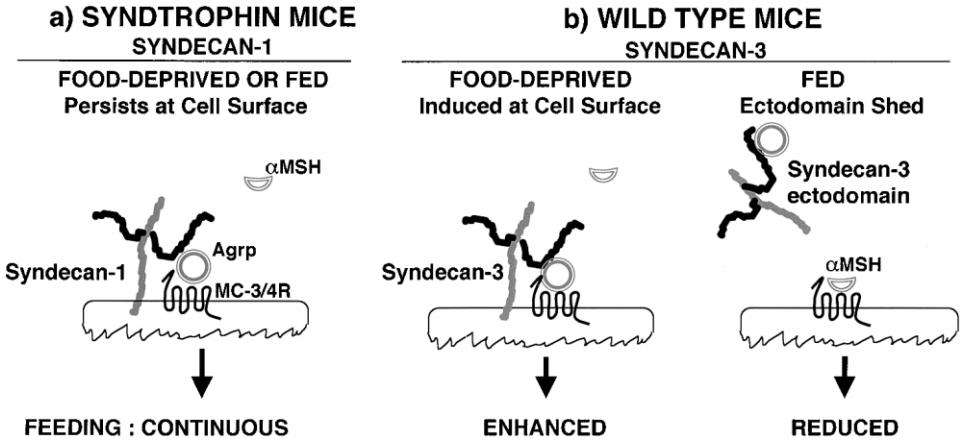

Figure 6. Model of Hypothalamic Postsynaptic Membranes Depicting the Role of Syndecans in Modulating Feeding Behavior

(a) In syndtrophin mice, misexpressed cell surface syndecan-1 persists at relatively high levels because of its inability to be shed. This results in constant potentiation of the activity of an antisatiety peptide, presumably Agrp at the MC-3R or -4R, producing continuous feeding and, ultimately, severe obesity.

(b) In contrast, in wild-type mice, cell surface syndecan-3 is induced in response to food deprivation and its ectodomain is shed in response to feeding. Thus, increased levels of cell surface syndecan-3 would potentiate the activity of an antisatiety peptide, presumably Agrp, and enhance feeding, whereas the shedding of the syndecan-3 ectodomain would remove this stimulus and reduce feeding. Syndecan core protein is presented as gray line and the covalently attached heparan sulfate chains presented as black squiggly lines.

site, in the vector, for the ISL-1 transcription factor. ISL-1 is expressed similarly as the syndecan-1 transgene in both brain and somatic tissues (Thor et al., 1991).

Action of Cell Surface Syndecans

Syndecans bind to the αMSH antagonists ASP and Agrp via their HS chains. Both cell surface syndecan-1 and -3 potentiate the inhibitory action of Agrp on the MC4-R, consistent with the physiological data implicating reduced αMSH action in syndtrophin mice and with the genetic interaction between syndtrophin and *lethal yellow* mice. The binding data suggest that the syndecan HS chains bind the N-terminal region of Agrp (Figure 3a), leaving the conserved C-terminal region free to interact with MC-3 or 4R, displace αMSH, and regulate feeding behavior (Hagan et al., 2000; Kiefer et al., 1998; Mizuno and Mobbs, 1999; Yang et al., 1999). These data are consistent with results that implicate the N-terminal region of the agouti proteins as the regulatory site (He et al., 2001; Nagle et al., 1999). By analogy to the coreceptor action of HSPGs in the formation of FGF-FGFR complexes (Rapraeger et al., 1991; Steinfeld et al., 1996), HSPG binding to Agrp likely augments formation of an Agrp-MC-3R or -4R complex, thus reducing access of αMSH to its receptor.

Syndecans must be at the cell surface to alter feeding behavior. Transgenically expressed hypothalamic syndecan-1 persists at the cell surface because it is not shed, resulting in continual inhibition of αMSH action (Figure 6). The level of transgenically expressed cell surface syndecan-1 correlates with weight gain (Figure 1b), whereas transgenically expressed constitutively shed syndecan-1 is without effect on body weight (Figure 4c). In contrast, hypothalamic syndecan-3 is both at the cell surface and shed as a soluble ectodomain, and its levels at the cell surface vary in response to feeding state. We propose that feeding is enhanced by increased levels of cell surface syndecan-3, and reduced when syndecan-3 is shed from the cell surface following food intake.

The processes responsible for the changes in syndecan-3 level are unknown. However, brain syndecan-3 has been shown to be induced, e.g., in long term potentiation (Lauri et al., 1998). Hypothalamic syndecan-3 is found as a mixture of soluble and cell surface HSPG, likely reflecting its release from cell surfaces by ectodomain shedding (Carey et al., 1997). Syndecan ectodomain shedding is highly regulated and involves cell surface receptors and various kinases impinging on a zinc metalloprotease (Fitzgerald et al., 2000). Multiple shedding enzymes have been identified to date and some have been shown to exhibit substrate specificity. Thus, it is likely that the shedding enzyme that cleaves syndecan-3 does not recognize syndecan-1 (Figures 4b and 5b). We speculate that activation of MC-3R or -4R neurons in response to a postprandial signal (e.g., insulin or amylin) causes a syndecan-3 specific metalloprotease to release the ectodomain from the cell surface (Figure 6).

Syndecans as Regulators of Peptidergic Synapses

More generally, our data add to the emerging evidence that syndecans are important in CNS synapses. Prior evidence has implicated syndecan-3 in the formation and guidance of CNS axons, in part by interacting with HB-GAM, an extracellular neurite outgrowth promoting peptide (Raulo et al., 1994). Syndecan-3 shares the C-terminal PDZ domain binding sequence EFYA with all other syndecans and various synaptic receptors, enabling them to bind CASK and other submembranous scaffolding proteins enriched in postsynaptic densities (Kennedy, 2000). Moreover, the accumulation and distribution of certain neuropeptides during CNS development is known to depend on synaptic cell surface HSPGs (Loeb et al., 1999). Finally, because there is no uptake mechanism or degrading system for neuropeptides in synaptic clefts (Kandel and Abel, 1995), ectodomain shedding would be a reasonable means of signal termination. Based on our evidence that syndecan-1 and -3 likely regulate MC-3R and -4R neurons, we suggest that cell surface HSPGs play regulatory roles in a variety of peptidergic synapses in the CNS.

Experimental Procedures

Construction of Syndecan-1 Transgenic and Syndecan-3 Null Mice

Syndecan-1 Transgenics

A full-length mouse syndecan-1 cDNA and mutant constructs were inserted into the HindIII site of the pCDNA3 plasmid (Invitrogen). Endonucleases MluI and DraIII were used to isolate a 2.5 kB fragment containing 660 bp of the CMV promoter, the syndecan-1 cDNA including 203 bp of its 3′UTR, and the 3′UTR and polyadenylation signal of bovine growth hormone. The fragment was injected into fertilized FVB oocytes and implanted into recipient pseudopregnant mice. Using PCR, a stop codon at aa S19 or Q245 was inserted for the nontranslatable or constitutive shed (CS) mutants, respectively. Multistep PCR replaced the juxtamembrane amino acid residues E238GATGASQSLLDTKE252 with the analogous region of human CD4, amino acid residues VKVLPTWSTRVQPMA for the uncleavable (UC) mutant. Transgenic offspring were identified initially by Southern blot analysis and routinely by PCR.

Syndecan-3 Null

Genomic sequence corresponding to syndecan-3 cDNA (Carey et al., 1997) was cloned from 129SV mouse genomic library (Stratagene). An 8.2 kb fragment containing exons 3–5 and a plasmid containing a PKG-neo and TK cassettes was used for generation of the targeting construct. A region from ApaI restriction site in exon 3 to BamHI restriction site downstream of the exon 4 was replaced by a PKG-neo cassette and the TK cassette was located to the 5′ end of the construct. Linearized targeting construct was electroporated into CJ7 ES cells (Swiatek and Gridley, 1993) and clones resistant to G418 and gancyclovir were selected. Targeting was confirmed by Southern hybridization with flanking probes. Cells from two independent clones were injected into C57BL/6 blastocysts. Chimeric animals were crossed to C57BL/6. Syndecan-3 gene product was not detected in −/− animals when tested by Northern hybridization, immunostaining, or Western analyses (Figure 5c).

Tissue Proteoglycan Extraction and Analysis

Tissues were isolated and homogenized using a polytron in a buffer containing 50 mM mannitol, 50 mM Tris (pH 7.4), 5 mM EDTA, and 1 mM PMSF. Homogenates were centrifuged at 1000 × g for 10 min and the supernatant spun at 100,000 × g for 30 min. The sediment was extracted for 1 hr at 4°C in a buffer containing 50 mM Tris (pH 7.4), 150 mM NaCl, 1% NP-40, 1% Tween-20, 0.5% Triton X-100, 5 mM EDTA, and 1 mM PMSF and centrifuged at 100,000 × g for 30 min to collect a detergent-soluble fraction. The supernatants were partially purified over Q-Sepharose columns and concentrated by three successive precipitations in 3 volumes of 96% ethanol containing 1.7% KAcetate. Samples were either untreated or digested with chondroitinase ABC, heparin lyase I, and heparin lyase III prior to PAGE. After transfer, immunoreactivity was detected

using monoclonal antibody 281-2 and the ECL method (Amersham). Alternatively, tissues were homogenized and extracted in buffer containing 0.32 M sucrose, 10 mM HEPES (pH 7.4), 5 mM EDTA, 1 mM EGTA, and Complete® protease cocktail (Boehringer Mannheim). Homogenates were centrifuged in at 5,000 × g to remove nuclei and cell debris, pellets were reextracted, and the supernatants centrifuged at 100,000 × g for 1 hr at 4°C. The supernatants were partially purified over Q-Sepharose. The pellets were extracted in a 4 Guanidine-HCl/50% buffered phenol/0.2 sodium acetate (pH 4.5) and extracted as described below.

Hypothalamic Proteoglycan Extraction and Analysis

Each individual hypothalamus was dissected from surrounding tissue (approximately 20 mg wet weight), extracted in 1 ml 4 M Guanidine-HCl, 50% buffered saturated phenol, 0.2 M NaAcetate (pH 4.5), and the samples rapidly vortexed for one minute. To this extract, a 0.2 ml $CHCl_3$/Isoamyl alcohol (IAA) was added and the sample centrifuged at 14,000 × g for 10 min to form aqueous and phenol phases. The phenol phase contains protein while the aqueous and interphase contain proteoglycans and nucleic acids. The phenol phase was discarded and the aqueous and interphase were reextracted twice in phenol and $CHCl_3$/IAA and subsequently precipitated with 3 volumes of 96% ethanol, 1.7% potassium acetate. Pellets were resuspended in Tris-buffered saline containing 0.5% Triton X-100 and reprecipitated several times to remove all traces of guanidine-HCl. Samples were digested with chondroitinase ABC and heparin lyase II and analyzed on SDS-PAGE. After transfer to cationic nylon membranes (Immobilon N, Millipore Corp), HSPGs were immunodetected using affinity-purified mouse syndecan-3 antibody and anti-stub antibody (3G10) kindly provided by Dr. Guido David (David et al., 1992). The GAG-free syndecan-3 ectodomain binds poorly to this and other types of membranes. Quantitation was performed using NIH Image version 1.60b7.

Feeding Studies

The food intake was measured in 6-week- and 6-month-old FVB or C57Bl/6J mice housed individually. After one week of acclimatization, mice were fed ad libitum for a two week period. Food was weighed daily to monitor for spillage. For food restriction studies, mice at 6 weeks of age were housed individually and provided an equivalent amount of chow (5.5 g chow/day) as consumed by the wild-type FVB mice, determined by the ad libitum food intake studies. Refeeding studies were performed on 12-week-old male mice acclimatized and housed as above. Food was removed for 16 hr, then the mice were refed and the chow remaining was weighed at the indicated times. Mice were weighed before initiation of food deprivation and of refeeding.

Immunohistochemical and In Situ Analysis

Mice were sacrificed by cervical dislocation and fixed by perfusion with 4% paraformaldehyde in phosphate buffered saline (PBS). The brains were dissected out, postfixed overnight at 4°C in 4% paraformaldehyde/PBS, dehydrated into xylene through a graded ethanol series and embedded in Paraplast paraffin (Oxford Laboratories). Sections were cut at 10 μm on a Reichert-Jung 2030 microtome and stored at 4°C.

Immunohistochemical analysis of syndecan-1 and oxytocin protein expression patterns was performed as follows: sections were deparaffinized in xylene and rehydrated into PBS through a graded ethanol series. Sections were blocked 1 hr in blocking buffer (0.5% caesin [I-Block, Tropix, Inc.] in PBS-T [PBS and 0.1% Tween-20]). Primary antibodies were diluted appropriately in blocking buffer and applied to the sections overnight at 4°C. The rat monoclonal antibody 281-2 against the murine syndecan-1 ectodomain (Jalkanen et al. 1985) was used at a concentration of 2.24 μg/ml. The affinity purified rabbit anti-mouse oxytocin (Phoenix Pharmaceuticals, Inc.) was used at 10 μg/ml. The 281-2 mAb was detected using a rat IgG 2a-specific secondary antibody conjugated to horseradish peroxidase at 1 μg/ml (Jackson ImmunoResearch Laboratories, Inc.) and the signal amplified using fluorescein-coupled tyramide amplification according to the manufacturer's (New England Nuclear) instructions. Oxytocin was detected by direct immunofluorescense using a rabbit IgG-specific secondary antibody conjugated to the fluorophore Texas Red at 10 μg/ml (Jackson ImmunoResearch Laboratories, Inc.). Confocal images were collected on a Zeiss LSM410/Zeiss Axiovert 135TV system. Fluorescein signal (488 nm) and Texas Red (586 nm) were collected sequentially on separate channels to avoid bleedthrough. Digital reconstruction and image processing was performed using Photoshop 6.0 (Adobe, Inc.).

Syndecan-3 expression in wild-type mice was performed as follows: adjacent sections were deparaffinized and blocked as described above. Primary antibodies were diluted appropriately in blocking buffer and applied to the adjacent sections overnight at 4°C. The affinity-purified rabbit polyclonal antibody against the murine syndecan-3 ectodomain was used at a concentration of 2 μg/ml. The affinity purified rabbit anti-mouse oxytocin (Phoenix Pharmaceuticals, Inc.) was used at 10 μg/ml. The primary antibodies were detected using a rabbit IgG-specific secondary antibody conjugated to biotin at 0.5 μg/ml and the signal amplified using the ABC-HRP method with diaminobenzidine/nickel according to the manufacturer's instructions (Vector Laboratories, Inc.). Images were collected by digital acquisition on a Zeiss Axioskop 2 system and processed using Zeiss OpenLab software and Photoshop 6.0.

In situ hybridization was performed using nonisotopic digoxigenin-labeled riboprobes on coronal brain sections. Antisense riboprobe specific for the murine syndecan-1 transcript produced specific staining relative to a control sense riboprobe controls, which gave no signal. To visualize the probe, an anti-digoxigenin alkaline phosphatase conjugated antibody was applied to the sections and the signal was detected by an 8.5 hr incubation with the BM purple substrate (Roche Biochemicals). Microscopy was performed on the Zeiss Axioskop 2 as described above.

Analysis of Plasma Constituents

Blood from living ad libitum fed mice was collected by puncture of the retro-orbital sinus with heparinized capillary tubes in siliconized microfuge tubes. Glucose levels were measured with 5 μl plasma using the glucose hexokinase assay (Glucose [HK] reagent [Sigma]). Insulin and leptin levels were measured with 25 μl plasma by specific radio-immunoassay with recombinant insulin and recombinant leptin as standards (Linco Research, Inc.). Corticosterone levels were measured with 5 μl plasma by a specific radio-immunoassay (ICN Diagnostics).

Ligand Blot Analysis

Varying concentrations of each peptide were bound to nitrocellulose membranes and confirmed by Ponceau S staining of the membrane. The membrane was then blocked with 1 mg/ml BSA in phosphate-buffered saline (PBS) for 1 hr at room temperature. [^{35}S]syndecan extracellular domain (5000 cpm/ml) was added, the membrane was incubated overnight at 4°C, washed several times with PBS, dried, and autoradiographed.

Melanocortin-4 Receptor Activation and Inhibition Analysis

HEK293 cells expressing human MC-4R were incubated with Agrp (1 nM) for 30 min and then stimulated with either 100 nM αMSH or NDP-αMSH and incubated an additional 30 min. Culture media were removed, 0.5 M formic acid was added to the cells, and samples analyzed using an cAMP EIA kit (Stratagene). To evaluate the action of syndecan-1 or -3, cells were transiently transfected with syndecan-1, -3, or control cDNA (nontranslatable syndecan-1 construct) using the Lipofectamine Reagent (GibcoBRL) and assayed as above. Assays were performed in triplicate.

Statistical Evaluation

All values are means +/− SEM. Two-tailed Student's t test was used to test for the significance of differences.

Acknowledgments

The authors would like to thank members of the Bernfield laboratory and Dr. Joseph A. Majzoub for advice, input, and critical reading of the manuscript. We would also like to thank Sharlene Yang for excellent technical assistance and Karen Strehlow for her initial work on the syndtrophin mice. This work was supported by grants from the National Institutes of Health (NIH) to M.B. (HD06763), J.

Volpe (HD18655), G.S.B. (DK28506), and from the Academy of Finland and the Technical Research Centre of Finland (Program of Molecular Neurobiology), and the Sigrid Juselius Foundation to H.K. G.S.B. is an Associate Investigator of the Howard Hughes Medical Institute. O.R. was supported by an individual NRSA from the NIH.

Received September 28, 1999; revised May 30, 2001.

References

Bagnol, D., Lu, X.Y., Kaelin, C.B., Day, H.E., Ollmann, M., Gantz, I., Akil, H., Barsh, G.S., and Watson, S.J. (1999). Anatomy of an endogenous antagonist: relationship between Agouti- related protein and proopiomelanocortin in brain. J. Neurosci. *19*, RC26.

Bernfield, M., Götte, M., Park, P.W., Reizes, O., Fitzgerald, M.L., Lincecum, J., and Zako, M. (1999). Functions of cell surface heparan sulfate proteoglycans. Ann. Rev. Biochem. *68*, 729–777.

Bray, G.A., and Tartaglia, L.A. (2000). Medicinal strategies in the treatment of obesity. Nature *404*, 672–677.

Carey, D.J., Conner, K., Asundi, V.K., O'Mahony, D.J., Stahl, R.C., Showalter, L., Cizmeci-Smith, G., Hartman, J., and Rothblum, L.I. (1997). cDNA cloning, genomic organization, and in vivo expression of rat N- syndecan. J. Biol. Chem. *272*, 2873–2879.

Cone, R.D., Lu, D., Koppula, S., Vage, I.D., Klungland, H., Boston, B., Chen, W., Orth, D.N., Pouton, C., and Kesterson, R.A. (1996). The melanocortin receptors: agonists, antagonists, and the hormonal contol of pigmentation. Recent Prog. Horm. Res. *51*, 287–318.

Conrad, H.E. (1998). Heparin-Binding Proteins (San Diego: Academic Press).

David, G., Bai, X.M., Van der Schueren, B., Cassiman, J.J., and Van den Berghe, H. (1992). Developmental changes in heparan sulfate expression: in situ detection with mAbs. J. Cell Biol. *119*, 961–975.

Fitzgerald, M.L., Wang, Z., Park, P.W., Murphy, G., and Bernfield, M. (2000). Shedding of syndecan-1 and -4 ectodomains is regulated by multiple signaling pathways and mediated by a TIMP-3-sensitive metalloproteinase. J. Cell Biol. *148*, 811–824.

Flier, J.S., and Maratos-Flier, E. (1998). Obesity and the hypothalamus: novel peptides for new pathways. Cell *92*, 437–440.

Friedman, J.M. (2000). Obesity in the new millennium. Nature *404*, 632–634.

Hagan, M.M., Rushing, P.A., Pritchard, L.M., Schwartz, M.W., Strack, A.M., Van Der Ploeg, L.H., Woods, S.C., and Seeley, R.J. (2000). Long-term orexigenic effects of AgRP-(83-132) involve mechanisms other than melanocortin receptor blockade. Am J. Physiol. Regul. Integr. Comp. Physiol. *279*, R47–52.

He, L., Gunn, T.M., Bouley, D.M., Lu, X.Y., Watson, S.J., Schlossman, S.F., Duke-Cohan, J.S., and Barsh, G.S. (2001). A biochemical function for attractin in agouti-induced pigmentation and obesity. Nat. Genet. *27*, 40–47.

Hooper, N.M., Karran, E.H., and Turner, A.J. (1997). Membrane protein secretases. Biochem. J. *321*, 265–279.

Hsueh, Y.P., and Sheng, M. (1999). Regulated expression and subcellular localization of syndecan heparan sulfate proteoglycans and the syndecan-binding protein CASK/LIN-2 during rat brain development. J. Neurosci. *19*, 7415–7425.

Huszar, D., Lynch, C.A., Fairchild-Huntress, V., Dunmore, J.H., Fang, Q., Berkemeier, L.R., Gu, W., Kesterson, R.A., Boston, B.A., Cone, R.D., et al. (1997). Targeted disruption of the melanocortin-4 receptor results in obesity in mice. Cell *88*, 131–141.

Jalkanen, M., Nguyen, H., Rapraeger, A., Kurn, N., and Bernfield, M. (1985). Heparan sulfate proteoglycans from mouse mammary epithelial cells: localization on the cell surface with a monoclonal antibody. J. Cell Biol. *101*, 976–984.

Kandel, E., and Abel, T. (1995). Neuropeptides, adenylyl cyclase, and memory storage. Science *268*, 825–826.

Kennedy, M.B. (2000). Signal-processing machines at the postsynaptic density. Science *290*, 750–754.

Kiefer, L.L., Veal, J.M., Mountjoy, K.G., and Wilkison, W.O. (1998). Melanocortin receptor binding determinants in the agouti protein. Biochemistry *37*, 991–997.

Lauri, S.E., Kaukinen, S., Kinnunen, T., Ylinen, A., Imai, S., Kaila, K., Taira, T., and Rauvala, H. (1998). Regulatory role and molecular interactions of a cell-surface heparan sulfate proteoglycan (N-syndecan) in hippocampal long-term potentiation. J. Neurosci. *19*, 1226–1235.

Loeb, J.A., Khurana, T.S., Robbins, J.T., Yee, A.G., and Fischbach, G.D. (1999). Expression patterns of transmembrane and released forms of neuregulin during spinal cord and neuromuscular synapse development. Development *126*, 781–791.

Lu, D., Willard, D., Patel, I.R., Kadwell, S., Overton, L., Kost, T., Luther, M., Chen, W., Woychik, R.P., Wilkinson, W.O., and Cone, R.D. (1994). Agouti protein is an antagonist of the melanocyte-stimulating-hormone receptor. Nature *371*, 799–802.

Mizuno, T.M., and Mobbs, C.V. (1999). Hypothalamic agouti-related protein messenger ribonucleic acid is inhibited by leptin and stimulated by fasting. Endocrinology *140*, 814–817.

Mountjoy, K.G., Mortrud, M.T., Low, M.J., Simerly, R.B., and Cone, R.D. (1994). Localization of the melanocortin-4 receptor (MC4-R) in neuroendocrine and autonomic control circuits in the brain. Mol. Endocrinol. *8*, 1298–1308.

Nagle, D.L., McGrail, S.H., Vitale, J., Woolf, E.A., Dussault, B.J., Jr., DiRocco, L., Holmgren, L., Montagno, J., Bork, P., Huszar, D., et al. (1999). The mahogany protein is a receptor involved in suppression of obesity. Nature *398*, 148–152.

Ollmann, M.M., Wilson, B.D., Yang, Y.-K., Kerns, J.A., Chen, Y., Gantz, I., and Barsh, G.S. (1997). Antagonism of central melanocortin receptors *in vitro* and *in vivo* by agouti-related protein. Science *278*, 135–138.

Palmiter, R.D., Erickson, J.C., Hollopeter, G., Baraban, S.C., and Schwartz, M.W. (1998). Life without neuropeptide Y. Recent Prog. Horm. Res. *53*, 163–199.

Park, P.W., Reizes, O., and Bernfield, M. (2000). Cell surface heparan sulfate proteoglycans: selective regulators of ligand-receptor encounters. J. Biol. Chem. *275*, 29923–29926.

Paxinos, G. (1995). The Rat Nervous System, 2nd Edition (San Diego: Academic Press).

Porte, D., Jr., Seeley, R.J., Woods, S.C., Baskin, D.G., Figlewicz, D.P., and Schwartz, M.W. (1998). Obesity, diabetes and the central nervous system. Diabetologia *41*, 863–881.

Rapraeger, A.C., Krufka, A., and Olwin, B.B. (1991). Requirement of heparan sulfate for bFGF-mediated fibroblast growth and myoblast differentiation. Science *252*, 1705–1708.

Raulo, E., Chernousov, M.A., Carey, D.J., Nolo, R., and Rauvala, H. (1994). Isolation of a neuronal cell surface receptor of heparin binding growth- associated molecule (HB-GAM). Identification as N-syndecan (syndecan-3). J. Biol. Chem. *269*, 12999–13004.

Salmivirta, M., Elenius, K., Vainio, S., Hofer, S., Chiquet-Ehrismann, R., Theslaff, I., and Jalkanen, M. (1991). Syndecan from embryonic tooth mesenchyme binds tenascin. J. Biol. Chem. *266*, 7733–7739.

Schwartz, M.W., Woods, S.C., Porte, D., Jr., Seeley, R.J., and Baskin, D.G. (2000). Central nervous system control of food intake. Nature *404*, 661–671.

Shutter, J.R., Graham, M., Kinsey, A.C., Scully, S., Luthy, R., and Stark, K.L. (1997). Hypothalamic expression of ART, a novel gene related to agouti, is up-regulated in *obese* and *diabetic* mutant mice. Genes Dev. *11*, 593–602.

Spiegelman, B.M., and Flier, J.S. (1996). Adipogenesis and obesity: rounding out the big picture. Cell *87*, 377–389.

Steinfeld, R., Van Den Berghe, H., and David, G. (1996). Stimulation of fibroblast growth factor receptor-1 occupancy and signaling by cell surface-associated syndecans and glypican. J. Cell Biol. *133*, 405–416.

Subramanian, S.V., Fitzgerald, M.L., and Bernfield, M. (1997). Regulated shedding of syndecan-1 and -4 ectodomains by thrombin and growth factor activation. J. Biol. Chem. *272*, 14713–14720.

Swiatek, P.J., and Gridley, T. (1993). Perinatal lethality and defects

in hindbrain development in mice homozygous for a targeted mutation of the zinc finger gene Krox20. Genes Dev. *7*, 2071–2084.

Thor, S., Ericson, J., Brannstrom, T., and Edlund, T. (1991). The homeodomain LIM protein Isl-1 is expressed in subsets of neurons and endocrine cells in the adult rat. Neuron *7*, 881–889.

Woods, S.C., Seeley, R.J., Porte, D., Jr., and Schwartz, M.W. (1998). Signals that regulate food intake and energy homeostasis. Science *280*, 1378–1383.

Yanagishita, M., and Hascall, V.C. (1984). Metabolism of proteoglycans in rat ovarian granulosa cell culture. Multiple intracellular degradative pathways and the effect of chloroquine. J. Biol. Chem. *259*, 10270–10283.

Yang, Y.K., Thompson, D.A., Dickinson, C.J., Wilken, J., Barsh, G.S., Kent, S.B., and Gantz, I. (1999). Characterization of agouti-related protein binding to melanocortin receptors. Mol. Endocrinol. *13*, 148–155.

Yaswen, L., Diehl, N., Brennan, M.B., and Hochgeschwender, U. (1999). Obesity in the mouse model of pro-opiomelanocortin deficiency responds to peripheral melanocortin. Nat. Med. *5*, 1066–1070.

Yen, T.T., Gill, A.M., Frigeri, L.G., Barsh, G.S., and Wolff, G.L. (1994). Obesity, diabetes, and neoplasia in yellow A(vy)/− mice: ectopic expression of the agouti gene. FASEB J. *8*, 479–488.